Contents lists available at ScienceDirect

Chemical Engineering Journal

journal homepage: www.elsevier.com/locate/cej

A facile blow spinning technique for green cellulose acetate/polystyrene composite separator for flexible energy storage devices

Amjid Rafique [a,*], Inês Sequeira [a], Ana Sofia Bento [a], Mariana Peyro Moniz [a], João Carmo [a], Eduardo Oliveira [a], João Pedro Oliveira [a], Ana Marques [a,b], Isabel Ferreira [a], Ana Catarina Baptista [a,*]

[a] CENIMAT|I3N, Materials Science Department, NOVA School of Science and Technology, SST NOVA 2829-516 Campus de Caparica, Portugal
[b] Physics Department, Faculty of Sciences, University of Lisbon, 1749-016 Lisbon, Portugal

ABSTRACT

The search of sustainable gadgets, such as the portable electronics and wearables, have sparked the need for more sustainable and environment friendly constituent elements (e.g., electrode materials, separators, and green electrolytes) and low-cost scalable fabrication techniques. Herein, a facile and scalable blow spinning technique is proposed for the synthesis of a cellulose-based separator for flexible energy storage devices. A cellulose acetate and polystyrene (CA:PS) based composite separator is synthesized for the first time for flexible supercapacitors by exploiting the blow spinning technique. Different combinations of CA:PS were synthesized, and electrochemical performances of the devices were evaluated. A sweat simulation solution is used as green electrolyte for the development of symmetrical carbon yarn-based supercapacitors. The influence on the device performances of pristine carbon yarn, activated carbon yarns and PEDOT functionalized carbon yarns, electrodes were compared. Specific capacitances of 2.8 Fg^{-1} and 33 Fg^{-1} were obtained for pristine carbon and PEDOT functionalized carbon fibers respectively. The fabricated devices exploiting the composite separator exhibited good washing stability up to 30 cycles and capacitance retention of 95% up to 1000 charge/discharge cycles.

1. Introduction

Electrochemical energy storage devices comprising supercapacitors, batteries and hybrid capacitors have attracted increasing interest in the past couple of decades, owing to their long cyclic life, safety, high energy, and power densities. These devices are potential power sources for electrical vehicles and portable electronic devices [1–3]. The quest of higher electrochemical performance has propelled an assiduous interest in materials, structural design and device configurations [4,5]. Significant progress in performance enhancement of the supercapacitors devices has been reported in the past decade particularly in terms of long cyclic life and more energy density. However, high cost of materials, safety issues, resource abundanceess and environmental benigness are still considered major challenges for the next generation of green and sustainable energy storage devices [6]. Currently a growing interests have been reported in cellulose-based components of electrochemical energy storage devices such as electrodes (anode & cathode) for batteries [7] and supercapacitors [8], current collectors [9], electrolyte [10]

and separators for batteries [11]. Nonetheless, development of low-cost separators as distinct parts from electrodes and electrolyte has attracted little consideration [12].

The function of a separator is to avoid physical contact between electrodes in order to prevent the short-circuiting of the device and ideally, it must exhibit key features such as: excellent chemical resistance, good mechanical strength (to meet device fabrication stresses), mild thickness, high level and uniformity of porosity to sustain harsh conditions (extreme weather conditions), thermal stability, excellent adsorption and retention of the electrolyte, as well as high ionic conductivity [13]. Currently, research focused on separators mainly exploited for lithium-ion based energy storage devices such as polyethylene (PE), polypropylene (PP), and their combinations [14] and glass fiber-based membranes, composite films and some nonwoven separators for fuel cells [12]. Therefore, there are fewer reports about separators synthesis and supercapacitors development [15] but even in these, separators are referred to have some shortcomings such as low surface hydrophilicity and uneven pore size distribution. Hence,

alternatives under investigation comprise cellulose-based separators.

Cellulose is a natural polymer material and just like polysaccharides, cellulose as a renewable, biodegradable, biocompatible, non-toxic, chemically modified and cost-effective biomass and its derivatives [16] are widely exploited in textile, paper, functional materials, biomedical fields and energy storage devices [17]. Jian et al., synthesized a bacterial cellulose-based nanofiber membranes and used them as separator for Li-ion batteries which exhibits good ionic conductivity, dimensional stability and comparable electrochemical performance [18]. Similarly, Liao et al., prepared a hydroxyethyl cellulose coated PP separators exploiting segregation induced self-assembly, demonstrating higher uptake of electrolyte, ionic conductivity and better cycling performance, than non-coated PP [19]. Cellulose acetate (CA) is a type of cellulose derived from cellulose and synthesized by reacting cellulose with acetic anhydride in the presence of a catalyst (i.e., sulfuric acid) [20]. CA is well-known as a biodegradable and biocompatible polymer. CA based nanofibers, owing to its environmental benign nature, have high potential to be exploited in different fields such as gas sensors [21], filtration [22], bone regeneration [23] and supercapacitors[24]. CA based composite separators are getting more attention recently in energy systems to cater the growing demand for portable electronics [25] that offer many advantages such as surface hydroxyl groups, excellent wettability, sufficient porosity, and good mechanical stability [26]. A large number of investigations are currently performed on tuning the porosity of the cellulose-based separators that can adsorb maximum electrolyte by making composites of cellulose with other polymers such as polydopamine/cellulose/polyacrylamide [27], CA/TiO_2 [28], PVDF/CA [29], PMMA/CA [30]. All these studies focused on the synthesis of porous structures based on cellulose derivatives but pore structure and other properties greatly depend on the preparation methods [15].

Porous cellulose films have been produced by electrospinning [31], force spinning [32], phase-inversion [32] and paper-making technique [33]. These techniques have complex preparation methods and poor control on parameters such as temperature and extrusion rates [15]. Electrospinning is the most widely used technique for fibrous membranes production and well-known from last three decades but still far from being applied widely at an industrial scale [15,34]. This is because of the low throughput of the technique; it is economically unviable for large scale production. Thus the new blow spinning technique has been proposed for producing the CA based nanofibers membranes [35]. Blow spinning technique enables electrospinning and melt-blow spinning for nanofibers synthesis and offers an advantage of ten times more throughput of nanofibers without high voltage requirement. This technique has been successfully employed to synthesize micro and nanofibers of polymers with a diameter ranging from few hundreds of nanometers to several microns depending on the experimental conditions [36]. Li et al., [37] have employed solution-based spinning to synthesize free-standing polyimide based membrane and used it for lithium-ion batteries which exhibited satisfactory porosity and remarkable thermal stability. Deng et al., [38] fabricated a cellulose and carboxylated polyimide based composite separator for energy storage applications which has shown excellent porosity and tensile strength. Polystyrene (PS) is an inexpensive and robust polymer that is extensively used in the plastic industry, filter media, ion exchanger and separator [39]. Furthermore, several studies have focused on PS as a composite material and the results demonstrated an enhancement in material performance compared to its counterpart [40]. Although many studies have been reported [41] for exploiting blow spinning for lithium-ion battery, to the best of our knowledge, there are no studies in the literature in which a CA based composite separator is synthesized using blow spinning for flexible supercapacitors.

In this paper, a simple and facile strategy is used to fabricate a cellulose/polystyrene based composite separator through the solution-based blow spinning technique. In this technique, the cellulose acetate and polystyrene based composite separator is directly deposited on flexible carbon yarn based electrodes and embedded of simulated sweat solution to work as electrolytes for flexible supercapacitors. The composite separators were optimized in terms of CA/PS ratio, and these separators exhibited remarkable charge transfer and excellent cyclic stability.

2. Experimental section

2.1. Preparation of carbon yarn-based electrodes

Commercial carbon yarns (TenaxTM-E HTA40 E13 3K200tex) were used as flexible current collector and as an active material, when functionalized with PEDOT conducting polymer after nitric acid activation treatment. While this activation improves PEDOT adhesion and also enhances the device electrochemical performance.

2.2. Surface functionalization of the carbon yarn

To increase the adhesion of the coatings, the fibers were submitted to several treatments. The first step was the washing of the fibers in acetone and ethanol in a 1:1 ratio and then a thermal treatment of the carbon yarns was performed at 450 °C for 45 minutes (min), with a heating ramp rate of 10 °C per min. After the treatment, the temperature was gradually decreased to room temperature at a cooling rate of 10 °C per min. The treated carbon yarn was washed again with acetone to remove impurities from the surface of the fibres and a dried at 80° C on a hotplate for 40 min. After all these processes, the carbon yarns were immersed into nitric acid (HNO$_3 \geq$ 65 %, Sigma-Aldrich) at a temperature of 80 °C for 16 hours (h) to recover the conductivity. After this nitric acid treatment, fibers were washed with deionized (DI) water until neutral pH was achieved. Then fibers were dried again at 80 °C on a hotplate.

2.3. PEDOT functionalization of yarn

After surface activation, the carbon yarns were coated with a PEDOT film by in-situ polymerization of EDOT, the monomer/oxidizing agent ratio, EDOT (monomer, Sigma-Aldrich) and $FeCl_3 \cdot 6H_2O$ (oxidizing agent, ChemLab NV), was 1:2 and the polymerization time was varied between: 2, 5, 10, 15 and 20 h. This protocol had already been used in a previous report [42]. The Ferric chloride was prepared by mixing 0.4 g of $FeCl_3$ in 10 ml of distilled water used as the oxidizing agent. Then, carbon yarns (~7 cm long and 180 μm thick) were immersed in the solution for 20 min. These yarns were next dried on the hot plate for 2 h at 50 °C followed by its insertion in the cap closed container with a 1.5 ml of EDOT aqueous solution. Finally, they were placed in the oven at 90 °C to functionalize the strands with PEDOT via in situ vapor phase polymerization. This process was repeated in the oven for different time e.g., 2, 5, 10, 15 and 20 h in order to optimize the polymerization process. For each polymerization time, three carbon yarn wires were functionalized at a time. At this point, the dark blueish PEDOT coated carbon yarns were obtained, cleaned throughly by consecutive washings with a deionized water–ethanol solution and finally were dried at ambient conditions.

2.4. Synthesis of the cellulose based composite separators

The composite cellulose-based separator was synthesized by blow spinning technique while testing different ratios of cellulose acetate (CA) and polystyrene (PS) (CA 20, 30, 40, 50, 60, 70 and 80%). A solution of 9% (m/v) each CA and PS are dissolved in N, N-Dimethylformamide (Merck) leaving the resulting solutions to stir overnight, until it become a homogeneous. These solutions were mixed with different CA/PS proportion: 20:80, 30:70, 40:60, 50:50, 60:40, 70:30, and 80:20 %. The resulting solutions were poured directly in the spray gun cup and the air pressure was fixed at 15 PSI. When the air flow was activated, the fibers of the cellulose composite separators were directly

deposited on the target. A glass substrate covered with thin aluminium foil was used as target to prevent static electricity, and the carbon yarns were attached to it. The use of controlled environment conditions (at a constant temperature of 90 °C) promotes the evaporation of the solvent which enhance the formation of fibres on the carbon yarn. The separator coated yarn threads were then removed from the target for device fabrication.

2.5. Electrolyte preparation

Simulated sweat solution (SSS) was prepared following a previously reported protocol (ISO 105-E04: 2013) [43] where by dissolving 0.05 g of L-histidine (Sigma Aldrich, 99 %), 0.5 g of sodium chloride (Sigma Aldrich, 99.5%), and 0.22 g of sodium phosphate monobasic (Fluka analytical, 90%) in 100 ml of ultrapure water (pH = 5.5) in the deionized water and SSS is then stored in the fridge.

2.6. Fabrication of supercapacitor device with twisted configuration

All the devices were fabricated using carbon yarn coated with CA/PS composite fibers curled up to 10 turns around the coated PEDOT functionalized electrode. Earlier, the electrodes were impregnated into SSS overnight. Before fabrication extra electrolyte was removed and 40 μl of SSS solution was used as electrolyte.

2.7. Morphological and chemical and mechanical characterization

The morphology of the samples was analysed by optical microscope (Leica DMi 8) and Scanning electron microscopy (SEM) (Hitachi S 2400). The chemical composition of the composite separator and that of the active material was investigated by confocal Raman spectroscopy (Witec Alpha 300 RAS) using a laser source with excitation wavelength of 532 nm. All spectra were acquired for 50 s while using a low laser power. For the analysis of the composite separator this was set to 0.6 mW and for the PEDOT coated yarns to 0.152 mW.

For the peeling test of the coating, a manual and mechanical method was used. In the manual method, a tape was glued to the surface of the yarn and then pulled from the surface of the electrode surface. The tape is ripped without controlling the force and velocity of the removal but the information about the detachment of the material could be obtained. The mechanical process on the tensile machine leads to better control of a tensile and velocity of pulling which was fixed at 5 mm/s.

The electrochemical analysis was performed by cyclic voltammetry measurements, galvanostatic charge and discharge and impedance spectroscopy using Gamry 1010 potentiostat/Galvanostate. All the measurements were performed in a symmetric electrode configuration of device in artificial sweat solution as electrolyte.

3. Results and discussions

Separators play a crucial role in conventional capacitors, supercapacitors, and other energy storage devices by separating the electrodes electrically and prevent their short circuits. A separator must have specific attributes to be used for energy storage systems such as porosity, good electrolyte affinity, chemical and thermal stability to ensure ionic conductivity of soaked electrolyte. Traditional separators (such as Polyolefin, polyethylene, polypropylene etc.) are considered hazardous and expensive material owing to high cost of raw material and synthesis techniques [44]. Due to these problems, natural resources-based polymers are considered potential materials for novel multifunctional devices because they offer biodegradability, non-toxicity, and potential to be adopted into circular economies. Cellulose acetate has attracted considerable attention thanks to its diverse attributes such as abundant availability, environmental benignes, non-toxicity and chemical stability. The pure cellulose separators are flammable and demonstrate high moisture content, limited porosity and limited surface

area which limit its applications in energy storage devices. Herein, Influence of processing parameters on the production of CA based membranes by blow spinning was first attempted with CA solution, but a film was formed instead a membrane of fibres. As such the influence of adding a certain amount of PS solution to the CA solution was studied. Polystyrene is a cheap polymer that is widely used in plastic industry and used as carrier to produce porous membrane structures and fibrous structure in blow spinning process [45]. PS is polymer matrix restrict the size of phase separation to molecular dimension due to chemical and physical linkages (covalent bonds and hydrogen bonding) between CA and PS [46]. Blending PS with CA polymer help not only in production of porous structure but also improve other attributes such as thermal stability, chemical and mechanical stability. Hence, solutions with different CA/PS ratios were tested as well as the influence of deposition time and gun-target distance. This study is detailed in supplementary information S1. Fig. 1a depicts a schematic representation of the entire preparation procedures from surface treatment and functionalization and fabrication of the supercapacitor devices. Fig. 1b shows a photograph of the spray cloud emerging from the airbrush during the blow spinning process and the corresponding spray pattern on the target (i.e., an aluminium coated glass substrate as shown in Fig. 1c). In the traditional spraying technique of the solution, compressed air atomizes the solution into a fine spray of liquid droplets. But when a polymer solution is used as precursor, the viscoelasticity of the polymer solution prevents the breakage of the stream into droplets. The trimming of the polymer occurs at the edge of the nozzle leading to growth of the stretched solution in shape of filaments. This stream of solution filaments moved in the axial direction by the high-speed gas flow, as observed in the Fig. 1b. The concentration and viscosity of the solution filaments keep changes owing to gradual vaporization of the solvent which eventually arrests the filaments in fibres. The conical shape dispersion of the fibres is observed near the target with a spray pattern shown in the lower part of the Fig. 1b.

Fig. 1 shows that on the target blow spinning provides symmetric spray deposited patterns with two distinct fibers distribution zones. While one is a dense zone, i.e., with a high fibers density and the other one is a dispersed fibers zone, i.e., it has a lower concentration of fibers. In the dense zone, the fibers are observed with random orientation while radially oriented extended flashes of isolated fibers are originating from the dense zone toward dispersed zone. According to Marchioli et al., [47] and Sow et al. [45] fibers in the vicinity of the wall of an airflow channel observed segregation and oriented in streamwise direction which depends on inertia and aspect ratios of the fibers. Therefore, it can be concluded that the radial outward flux of the compressed air is responsible for the radial orientation of the stretched streaks of the segregated fibers. Fig. 1d shows that target carbon yarn is uniformly covered with the composite separator for all the ratios as shown in the digital images (S3 supporting information). SEM images Fig. 1e and 1f show the fibrous morphology of the synthesized separator on the carbon yarn confirming the viability to fabricate fibrous membrane from CA/PS system exploiting blow spinning technique. Fiber melting was also noted for blow spun membranes as shown in the SEM image Fig. 1e.

Some of the fibers were observed to be melted at single node and rest majority of the stretched streaks of fibers were soldered together along the 1D orientated bundles. The melt process advances by solvent-based re-dissolution and ultimately solidification. This demonstrated that this process is primarily happening during the fiber streaks flight when the fibers include some un-evaporated solvent and get in contact with each other. Fig. 1f shows the presence of micropores on the surface of the fibers. Similar pores distribution has also been found to exist on the surface of electrospun fibers under high relative humidity conditions [48]. Similar to the electrospinning technique, their formation is also expected in blow spinning process which results from polymer-solvent interactions in moist air [49]. Fig. 2a shows a schematic of the functionalization process of the carbon yarn with PEDOT polymer. The carbon yarns comprise of multi-filaments of the carbon fibers with an average diameter of 6 μm each and demonstrated an exceptionally
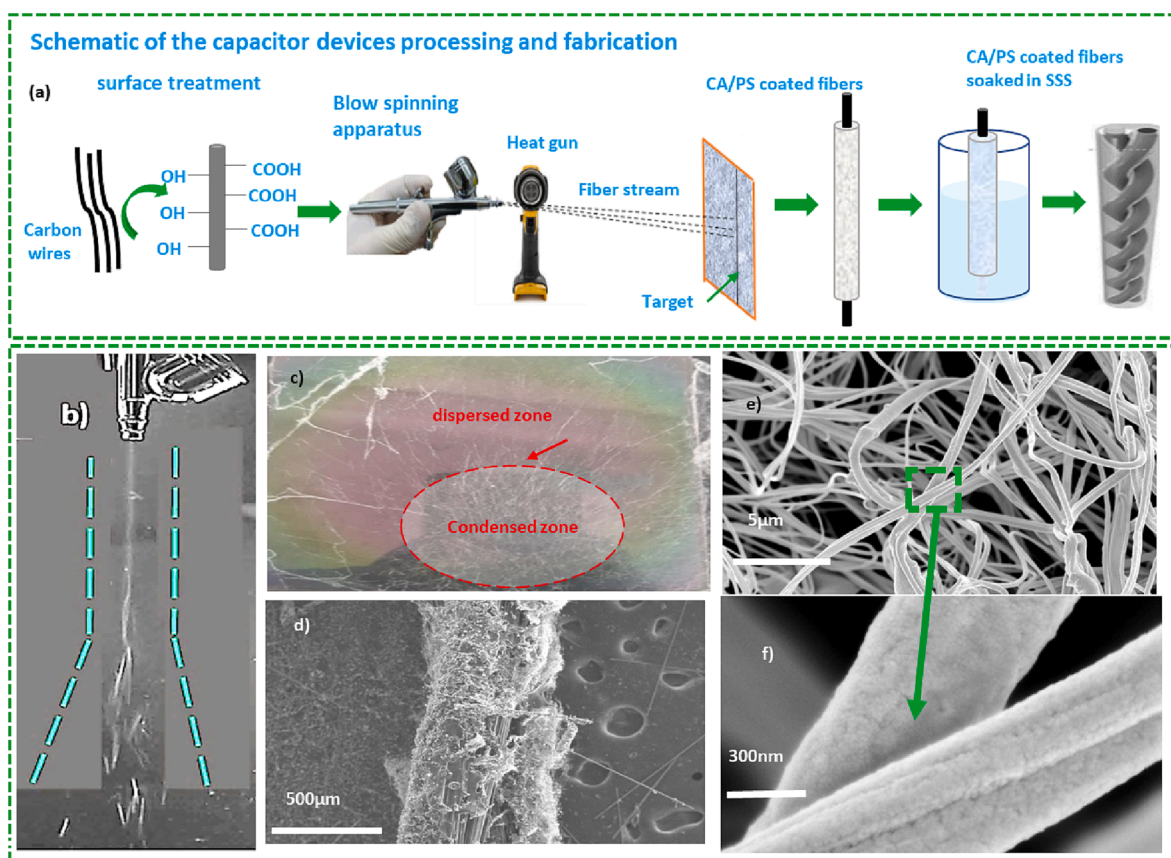
Fig. 1. a) Schematic illustration of cellulose acetate-based composite separator synthesis, b) optical image of spray plume while blow spin process, c) Optical image of spray collected on glass target, d) CA/PS base composite separator deposited on carbon yarn, e-f) high-magnification SEM image of the composite separator.

smooth surface as shown in Fig. 2b. After the carbon yarns were subjected to in-situ polymerization, Fig. 2c-d exhibit the resulted hydrothermally coated CF electrodes, which visibly demonstrated the growth of 2 and 10 h PEDOT nanocoating over their surface. The SEM image of bare carbon yarn refer to Fig. 2b and coated yarn are shown in Fig. 2c and 2d, detail the smooth surface of the carbon fibres. The SEM images in Fig. 2c-e clearly demonstrate the uniform coverage of carbon fibers with PEDOT nanostructure nearly leaving any uncoated area. It is also clear in Fig. 2 e the even distribution of the PEDOT nanostructures over carbon fibers which is expected to provide higher surface area to the carbon yarn electrode. The 3D morphology of deposited structure is beneficial for ions intercalation/adsorption [50]. The SEM morphology of the separator is depicted in Fig. 2g. The pore size of the composite separator was analysed using ImageJ (1250 pores were measured randomly). The average pore size of the separator is 15 μm.

As will be shown in electrochemical section, the composite cellulose-based separators with increasing percentages of CA in the composition, have negligible effects on electrochemical performances of the devices. Therefore, the chemical composition of a single CA based green separator was investigated by Raman spectroscopy. Fig. 3a shows the Raman spectrum acquired for the separator synthetized with a CA/PS ratio of 80%:20%. From top to bottom it presents the raw materials (CA and PS) and the 80% CA:20% PS composite separator spectra.

This is a linear combination of both raw materials spectra with no other contaminant phases detected as shown in Fig. 3a which is further highlighted by arrow pointing some characteristic functional groups of CA and PS in the composite separator spectrum. The main characteristic peaks corresponding to CA and PS vibrational modes are listed in Table S2 and identification is according to literature [51]. Also, the carbon yarns coated with PEDOT to form the supercapacitor electrodes were further investigated by Raman spectroscopy. The aim was to study

the effect of polymerization time on the PEDOT coating compositions, thickness, and structure, as the coating method relied on the oxidative polymerization of EDOT monomer. Fig. 3b shows the Raman spectra of the carbon yarn before (top) and after polymerization (bottom) as a function of its duration. The carbon yarn spectrum shows as previously reported the two characteristic D and G bands centered at 1367.87 and 1592.24 cm^{-1} [52]. The PEDOT spectra confirms that the surface of the carbon electrodes was successfully coated with PEDOT regardless of the polymerization time. The main bands assignments have been made considering the data reported in the literature [53,54] and are summarized in Table S3. The most intense peak was always detected at 1437.88 cm^{-1} and it corresponds to the $C_{\alpha}=C_{\beta}$ symmetric stretching vibration of the PEDOT benzoid structure. As it is shown, its intensity strongly correlates with polymerization time and hence, with the amount of PEDOT on the electrodes surface and consequently, also with PEDOT coating thickness. This should be thin for polymerization times below 10 h, because vibration bands at wavenumbers lower than 1000 cm^{-1} are hardly visible. Besides, the most intense detected bands at around 1200–1600 cm^{-1} seem to have poorer crystallinity as the corresponding peaks are broader. Also, SEM images confirmed that although a polymerization time equal or above than 2 h is enough to uniformly cover the supercapacitors electrodes with PEDOT, they also show that its morphology is polymerization time dependent, and which may would have impact on the device's electrochemical performance. The carbon yarns are functionalized with PEDOT exploiting in-situ polymerization for different time such as 2, 5, 10, 15, and 20 h respectively. After performing polymerization, conductivity of the carbon yarns and also adhesion of the polymer film was evaluated using peel-off test (detail shown in supporting information). The results are shown in Fig. S4(b) suggesting that PEDOT coating is well adhered to the surface of carbon yarn for polymerization times higher than 10 h. For
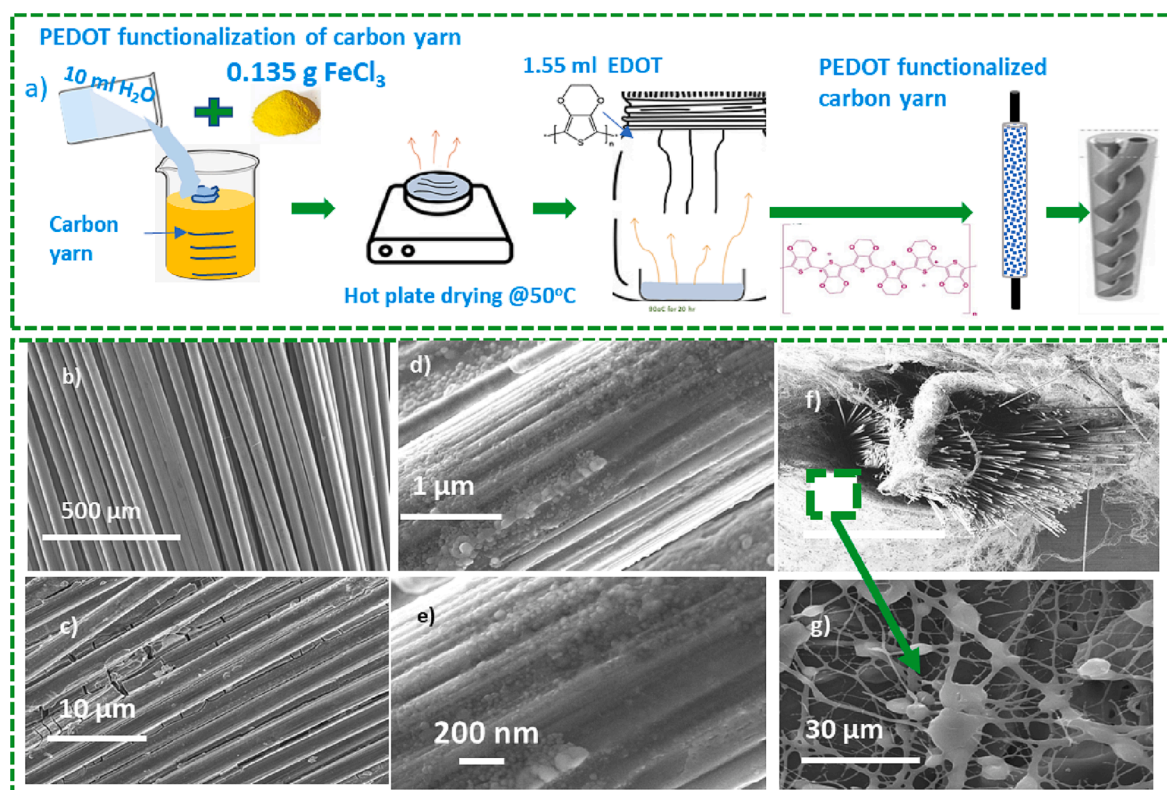
Fig. 2. Schematic of in-situ polymer functionalization of carbon yarn with PEDOT, b) SEM image of pristine carbon yarn, c-d) SEM image of 2 and 10 h PEDOT coated carbon yarn, e) higher magnification images of PEDOT coated carbon yarns, f) carbon yarn uniformly covered with CA/PS based composite separator, g) higher magnification image of the composite separator.
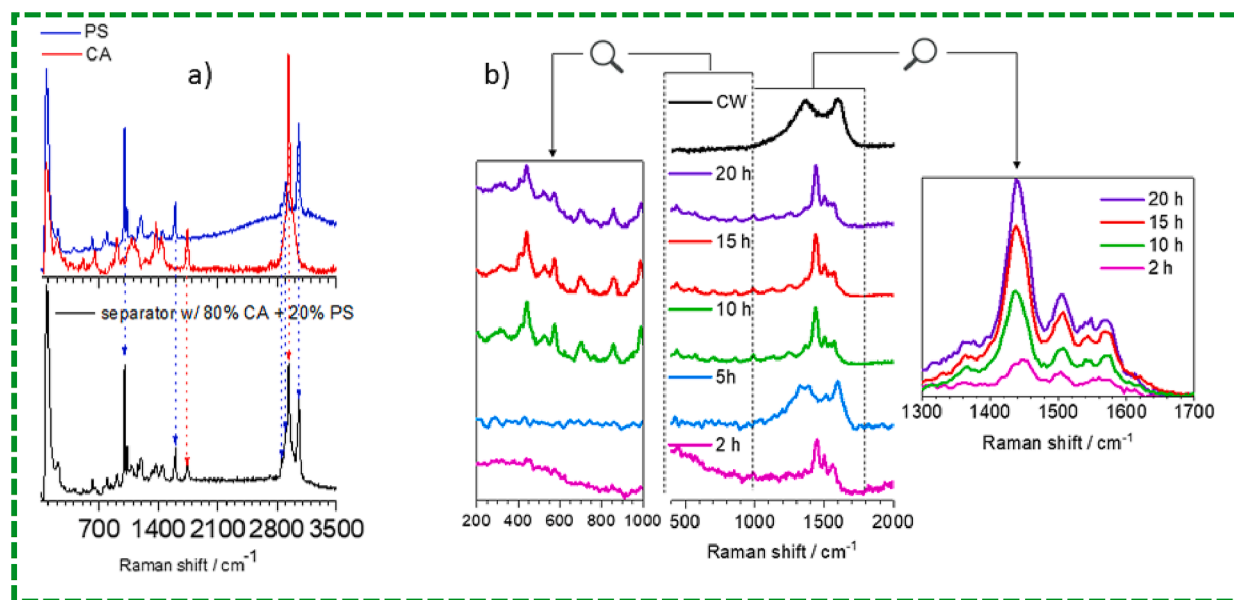

Fig. 3. a) From (top) to bottom Pristine (cellulose acetate - CA and polystyrene - PS) and composite separator (80%:20% CA:PS) Raman spectra, b) From top to bottom carbon yard Raman spectra before (black) and after performing PEDOT polymerization for different time intervals.

polymerization times above 10 h, it was observed that the peeling-off testing promoted the break of some carbon filaments from the core of carbon yarn affecting the conductivity values (polymerization time of 2 h) or an easy detachment of PEDOT coating polymerization time of 5 h. To conclude, a polymerization time of 10 h was selected to proceed with the assembly of supercapacitors.

Potassium hydroxide, Na_2SO_4 and H_2SO_4 were used as aqueous and

gel-polymer in combination with polyvinyl alcohol (PVA) are the most used electrolytes for flexible supercapacitors due to their excellent conductivity. However, for supercapacitors integrated on textiles, it may be a risk since leakage of electrolyte can causes safety issues due to their toxicity. To avoiding these safety issues, we have studied the possibility to used human sweat solution as electrolyte. Human body sweat comprised various chemicals such as amino acids, proteins, lipids and

except for ionic species, most of the constituent elements in the sweat solution are neutral and have almost no interference in ionic conductivity [55]. Artificial sweat solution was tested in the electrochemical characterization of the fabricated devices. Before performing the electrochemical analysis of the devices and study electrochemical behavior of the composite separator, electrolyte affinity and porosity tests were performed to estimate the amount of electrolyte absorbed by the composite separators (see detailed procedure and mathematical model in supporting information). The separator exhibited a relative porosity of about 59 % for each composite separator membrane prepared with different CA and PS ratios, which are comparable to other cellulose-based separators and higher than traditional separators as shown in the Table 1. In order to investigate the long-term stability of the CA based composite separators, the electrolyte uptake and swelling of separator membrane was calculated by immersing the separator in simulated sweat solution at room temperature for 48 h. Then, the mass and area changes of the samples after different storage time to compute the stability of the separators was measured, using the mass of the separator W_o before soaking and W_1 after 48 h soaking. The calculation was performed according to the equation(S2) and electrolyte absorption of different CA-based composite membranes were compare with each other as shown in the Fig. 4a and b. The comparison was also performed with other cellulose-based separators and with traditional material such as polypropylene and PVDF based separators.

The thickness of the blow spun CA based composite separator is evaluated by measuring the thickness at three different points of flexible separator coated wires namely right, middle and left corner of the electrode. The average thickness of the separator around the wires is measured and these results are compared as shown in the Fig. 4c and d. It is clear that the electrodes are uniformly covered with composite separators with an average thickness of 1.2 mm.

Electrochemical measurements were performed using symmetrical two electrode configurations in simulated sweat solution as electrolyte to evaluate the capacitive performance through cyclic voltammetry, galvanostatic charge/discharge and specific capacitance. Different combinations of device fabrications were studied with pristine carbon fibers, activated carbon fibers and conductive polymer functionalized carbon fibers. Different devices were fabricated for all the studied CA:PS ratios of composite separator and the CVs recorded at 100 mVs⁻¹ scan rates, between voltage window from 0 to 1 V, are shown in Fig. 5b. All the CV curves exhibit nearly rectangular shape with no distinct redox peaks which demonstrates an ideal and efficient nature of electric double layer capacitor(EDLC), and for pure carbon-based active material [65] the variation on the composition of membranes does not show a considerable influence. Fig. 5c is shows the CVs of devices performed with activation of the carbon wires as activation details described in the experimental section. The electrochemical response of these devices

deviate from the ideal EDLC behavior in which shape of the CVs is lifted upward [66]. This is a symptom of a slow charge transfer process in which charging and discharging response delayed by the potential difference across micropores [67]. This is attributed to the faradaic process involved in charging and discharging, and functional group present on the surface of the electrode and material exhibits pseudocapacitive behavior [68], which in turn increases specific capacitance of the device as demonstrated in Fig. 5d-e. Since, all the composite separators demonstrated negligible variability in electrochemical performance, 80%:20% CA:PS ratio was chosen as green separator to evaluate electrochemical performance. Fig. 5 d shows the CVs recoded at different scan rates and the capacitance of the cell is also calculated using the following relation [69],

$$C_{cell} = Q/_{2V} = \frac{1}{2V\nu} \int\limits_{v-}^{v+} i(V)dV \tag{1}$$

where C_{cell} is the capacitance of the cell, i is the current, ν is the scan rate, V (V = V₊ - V₋) described the potential window. Specific capacitance is computed using equation (2),

$$C_{sp} \text{ (F/g)} = C_{cell} /m \tag{2}$$

where m denotes the mass of the electrodes.

The specific capacitances of activated carbon fiber (ACF)//ACF, PEDOT/CF//CF and PEDOT/CF// PEDOT//CF supercapacitors were computed using two electrode configurations in SSS as electrolyte and 15 cycles were recorded for each configuration. The specific capacitance was computed for every 14th cycle. Fig. 5e show the specific capacitance at different scan rates and highest specific capacitance of 2.28 Fg⁻¹ achieved at 30 mVs⁻¹. However, as we increase the scan rate, specific capacitance decrease at rapid rate owing to a incomplete EDLC formation [52]. Fig. 5f shows the galvanostatic charge and discharge (GCD) curves for activated carbon wires-based supercapacitors with CA 80% separator at different current densities ranging from 1.25 mAg⁻¹ to 30 mAg⁻¹. The GCD curves nearly triangular shape with some distortion of from ideal EDLC which is attributed to the pseudocapacitive behavior of the material. This pseudocapacitive behavior is more pronounced at lower current densities ascribed to faradaic reactions taking place during charge and discharge. It is also worth noting that no obvious IR (ohmic drop) drop is observed even at lower current density which indicates a relatively low internal resistance. This can be attributed to faster charge transfer and ion diffusion ability supported by CA based separators. CV curves are also obtained for PEDOT functionalized carbon fibers in PEDOT/CF//CF and PEDOT/CF//PEDOT/CF configurations with CA:PS 80%:20% as separator. The CV curves for the fabricated devices are recorded for different scan rates. The CVs demonstrated a symmetric reversible quasi-rectangular shape from 5 to

Table 1
Comparison of electrolyte affinity and porosity of traditional and cellulose-based separators.

| Sr#	Separator	electrolyte	Technique	Porosity (%)	Electrolyte affinity (%)	Ref.
1	Polypropylene	n-butanol	–	39.2	62.9	[56]
2	PVDF	n-butanol	Electrospinning	75	405	[56]
3	PVDF/Al₂O₃	n-butanol	Electrospinning	55.8	152	[56]
4	PVDF-CA	Li/GPE/LiCoO₂	Electrospinning	52	331	[57]
5	Cellulose/PVDF-HFP	LiPF6 in EC/DMC	Electrospinning	65	186	[58]
6	Cellulose	LiPF6 in EC/DMC	Vacuum assisted filtration	26		[59]
7	Cellulose	LiPF6 in EC/DMC	Paper making technique	63.8	333	[60]
8	Nano fibrillated cellulose (NFC)	LiPF6 in EC/DMC	Solvent casting and vacuum	57		[61]
9	Cellulose diacetate	LiPF6 in EC/DMC	Solvent casting by dip coating	41	277	[62]
10	Carboxyl methyl cellulose	LiPF6 in EC/DMC	Doctor blade casting	62.5		[63]
11	Mesoporous cellulose	LiPF6 in EC/DMC	Solvent casting with evaporation induced self-assembly	75	280	[64]
12	CA: PS 80%: 20%	Artificial sweat solution	Blow spinning technique	**59**	**251**	**This work**
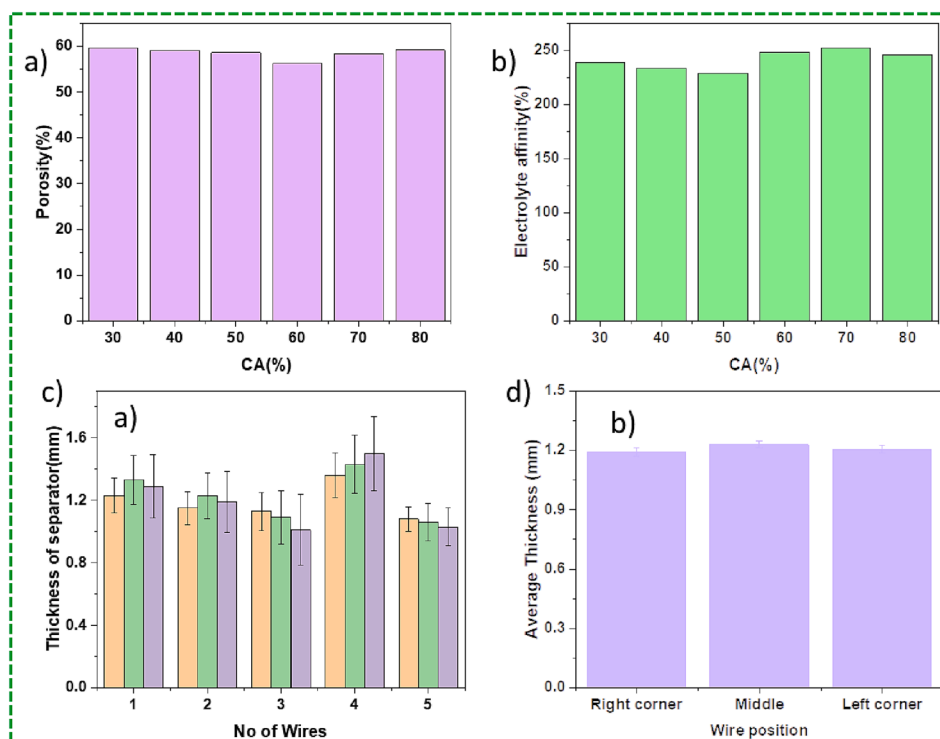
Fig. 4. a-b) Comparison of porosity and electrolyte affinity of different ratios of CA based composite separators, c-d) thickness and uniformity of composite separators deposited on carbon wires at different position of electrode and average of thickness.

100 mVs^{-1} and fast ions transportation as shown in Fig. 6a-d. The total charge stored by conducting polymers (PEDOT/CF) composite electrode material can be divided into parts: i) surface adsorption/desorption of ions of electrolyte with composite electrodes and their reaction can represented as follows:

$$PEDOT/CF) \text{ surface} + C^+ + e^- \leftrightarrow (PEDOT/CF^+) \text{surface} \qquad \text{i)}$$

ii) The second mechanism of charge storage is intercalation of cations (C$^+$) into bulk of the composite electrode material as referenced in the Eq. ii):

$$PEDOT/CF + C^+ + e^- \leftrightarrow PEDOT/CF \qquad \text{ii)}$$

Here C$^+$ denotes the cations from electrolyte (sweat artificial solution). In addition, the conductive and exposed inner pores of the electrode surface support the movement of the electrolyte's ions which accumulate at an increased number of free active surface sites of the material. The electrochemical charge accumulation process includes surface adsorption and desorption of counter-ions in and out of the PEDOT polymer chain which effectively lean on ion diffusion, surface area of the material and conductivity of the PEDOT electrodes. Mitraka et al., and Libu et al., have improved the capacitive performance of the PEDOT conducting material in artificial sweat solution and combination of artificial solution with other electrolytes [70–72]. Cations from the sweat electrolyte (Na$^+$ or K$^+$) enter the PEDOT:PSS channel and the oxidized PEDOT$^+$ can be reduced to its natural state by ions exchange with the sweat electrolyte as shown in equation ii). PEDOT conductive polymer is suitable as an active material for electrode fabrication owing to availability of free electron sites which promote specific preferred reaction pathways. Moreover, there is no protective layer coverage along the electrode–electrolyte interface which then becomes a vibrant interface for charge transfer in the SCs device. The electrode–electrolyte interface system distinguishes PEDOT from other heterogeneous electro catalysts, which allows the PEDOT based composite material reachable by neutral and ionic reactants. The presence of high positive charge density in bulk of PEDOT phase play a significant role for conductivity

and charge accumulation of anions [73]. This improvement in conductivity is observed in specific capacitance, when compared to activated fibers which is 10 Fg^{-1} and 33 Fg^{-1} at 5 mVs^{-1} respectively. This increase in specific capacitance ascribed to enhanced surface area which offers more active sites for electrolyte ions during faradaic reactions indicating possible pseudocapacitive behavior of the PEDOT. These results show better performance than other separators in the same artificial sweat electrolyte such as functionalized carbon covered with electrospun cellulose acetate separator by Lima et al. with specific capacitance of 2.3 Fg^{-1} [52], PEDOT:PSS functionalized Polyester/cellulose electrode covered Polyester/cellulose substrate with specific capacitance of 5.65 Fg^{-1} and PEDOT: PSS functionalized Polyester/cellulose covered with cellulose fibers separator with specific capacitance 2.9 Fg^{-1} by Manjakkal et al. [70,71]. The devices assembled with composite separator exhibited comparable performance with other separators as shown in Table 2.

The electrochemical properties of the supercapacitors which include ion exchange, charge transfer and capacitance were computed by impedance spectroscopy analysis in the frequency range of 10 mHz to 100 kHz. The Nyquist plot for the composite separators coated carbon yarns with different CA ratios in the sweat electrolyte are shown in Fig. 6e. Nyquist plots are also obtained for PEDOT functionalized carbon yarn-based supercapacitors devices (PEDOT-Cf//CF, PEDOT-Cf//PEDOT-CF) in sweat electrolyte as shown in Fig. 6f. In the low frequency range, the impedance decreases sharply with increasing frequency and a plateau is noted at high frequencies. The straight line in the low range frequency of the Nyquist plot indicates the slower diffusion of ions into the active material and the capacitive behaviour of carbon yarn wires-based supercapacitors. The absence of semi-circle in high frequency range in Nyquist plot and the small value of charge transfer resistance (Rct) exhibit the high conductivity of the electrode. The PEDOT functionalized electrodes in symmetric and asymmetric configurations exhibited comparable or slightly higher resistance than when tested in asymmetric configuration owing to high amount of PEDOT in symmetric devices with resistances of 28 Ω and 31 Ω and
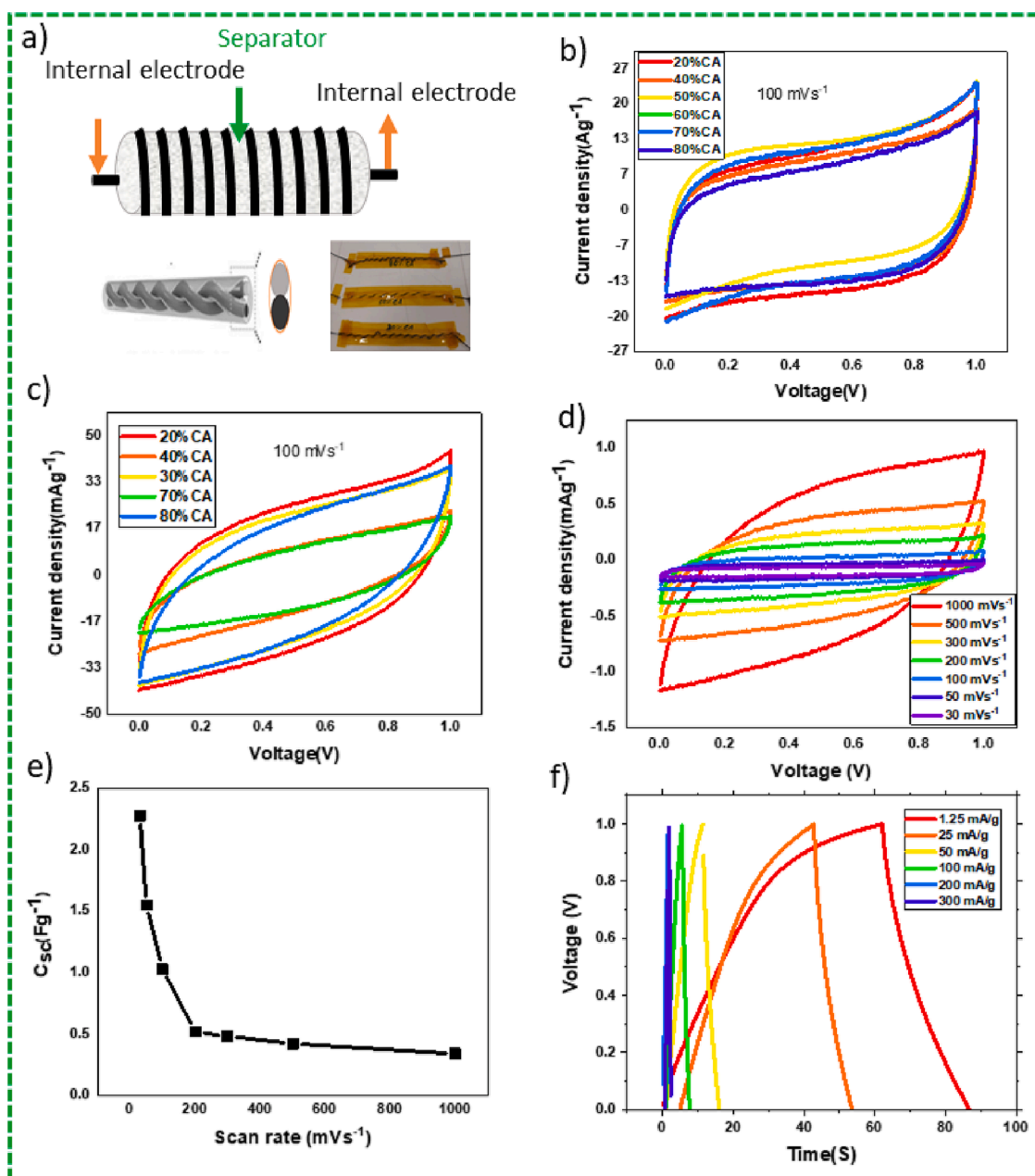
Fig. 5. a) Schematic view of the device fabrication and fabricated device (inset below), b and c) CV curves comparison of all separators pristine and activated carbon fibers, d-e) CVs comparison recorded at different scan rate for CA: PS 80%:20% and specific capacitance, f) galvanostatic charge and discharge comparison at different current densities.

corresponding charge transfer resistance of 78 Ω and 81 Ω respectively.

During practical application, flexible electronic devices are subjected to different mechanical type of loading and therefore flexible electronic devices and supercapacitors must sustain bending, twisting, and tensile stresses. The flexibility and bending stability of the devices were measured by performing electrochemical analysis with the device bent at different angles (0°, 30°, 60°, 90°, 120°, 150°, and 180°) and the fabricated device demonstrated excellent bending stability with capacitance retention of above 98 % as shown in the Fig. 7. The cyclic voltammograms were also recorded in the flat position after these bending stress levels were applied and the device almost fully recovered its default capacitance. These demonstrations complement the suitability of easy integration of these separators coated devices into textiles, owing to the high bending stability and capacitance retention. This attribute also demonstrates that the device can clearly withstand the mechanical

stresses during traditional weaving process necessary for textile integration and during wearability.

Device connection in series or parallel is a necessity for power supply to electronic devices and for their practical applications. Devices are also connected and stacked in series and parallel configuration. The flexible strip-shaped supercapacitors can be further integrated for high energy and power capabilities by connecting in series and parallel. For instance, the voltage windows linearly increased with the increasing number of supercapacitors being connected in series as shown in Fig. 8a-b. The specific capacitance can be enhanced by connecting them in parallel. As shown in Fig. 8c and d, both the discharge time and output current increased by three times when three supercapacitors were connected in parallel configuration. The voltage profiles and of the CVs were perfectly retained, indicating that the connected devices steadily performed without degradation. Furthermore, the capacitances linearly increased
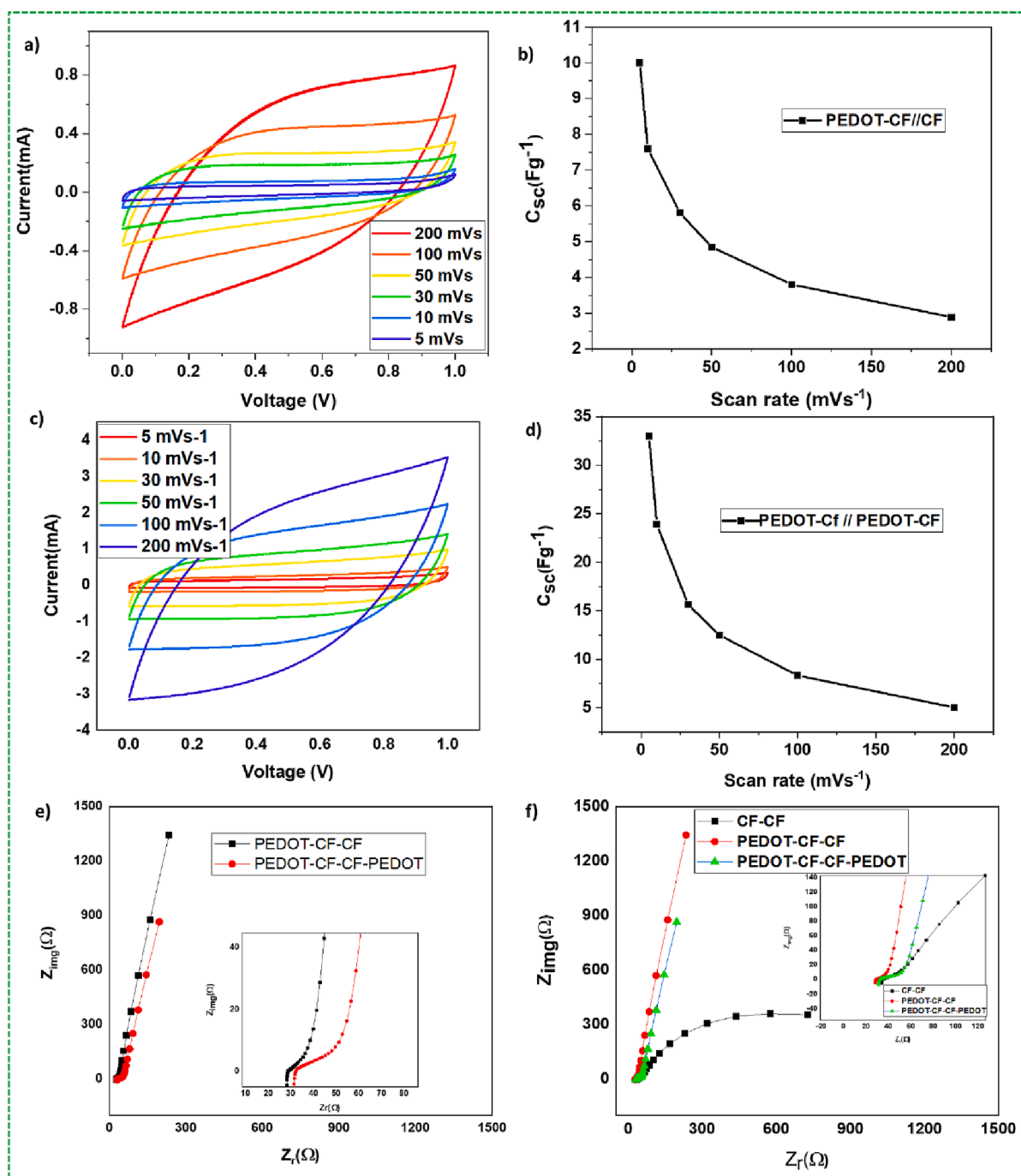
Fig. 6. a-b) CVs comparison recorded for inner PEDOT functionalized carbon wires electrodes and outer electrode carbon fibers and corresponding specific capacitances at different scan ates, c-d) CVs comparison for PEDOT functionalized electrode (inter & outer) and corresponding specific capacitances comparison at different scan rate, e-f) impedance spectroscopy spectra of PEDOT functionalized carbon yarn and its comparison with pristine carbon yarn.

with the increasing number of supercapacitors. As the photograph inserted in Fig. 8 shows, a red LED is lighted by connecting devices in parallel and series. This is an efficient way to exploit flexible supercapacitors as steady sources of energy output devices by connecting them in series and parallel configurations. These results indicate that it might be an available approach to monitor the operating voltage and current by employing series and parallel configurations with slight energy losses. A video of LED lighting demonstration is attached in supporting information appended to this work.

E-textile during practical application subject to many stress levels such as abrasion resistance and washing resistance. Wearable devices and e-textiles must sustain these stresses during wearability and washing

process. Abrasion resistance is the ability of the fabric to resist to the surface wear of the device integrated in the textile caused by the flat rubbing contact with another material. As per ASTM standards, there are two different methods commonly used by the textile industry to assess abrasion resistance, namely Whyzenbeek (ASTM D4157-07) and Martindale testing method (ASTM D4966-98). We have used both methods with specific modifications to evaluate the abrasion resistance of the devices because both of these test methods are used to measure flat abrasion resistance of a textile in the industry. It should be mentioned that there is no correlation between these two methods. The devices were integrated into the textile and abrasion tests were performed after different sets of rotations were imposed, as shown in Fig. 9a. After

Table 2
Comparison of flexible supercapacitors performance with CA based devices in artificial sweat electrolyte.

| #	Material	Electrolyte	Substrate	V. W	Separator	Capacitance Fg^{-1}	Energy density $(mWhkg^{-1})$	Power density Wkg^{-1}	Ref.
1	Func. CY	Artificial Sweat Solution	Carbon yarn	1	Electrospun Cellulose Acetate	2.3	386	0.046	[52]
2	PEDOT: PSS	Artificial Sweat Solution	Polyester/cellulose	1.3	Polyester/Cellulose	5.65	1360	329	[70]
3	carbon	H_2SO_4	Stainless steel		Eggshell membrane	2.3			[74]
4	PEDOT: PSS	Artificial Sweat Solution	cellulose/polyester cloth	0.8	Cellulose fibers	2.9			[71]
5	mesoporous carbon	EmimTFSI	stainless-steel	3.5	Pullulan	18	7200	4600	[75]
6	MWCNT	PEO/LiCl	Micro fibrillated cellulose (MFC)		Microfibrillated Cellulose	154.5 $mFcm^{-2}$			[76]
7	PEDOT/CY-PEDOT/CF	Artificial Sweat Solution	Carbon yarn	1	Blow spun Cellulose Acetate	33	4046	292	**This work**
8	PEDOT/CY-CY	Artificial Sweat Solution	Carbon yarn	1	Blow spun Cellulose Acetate	10			**This Work**
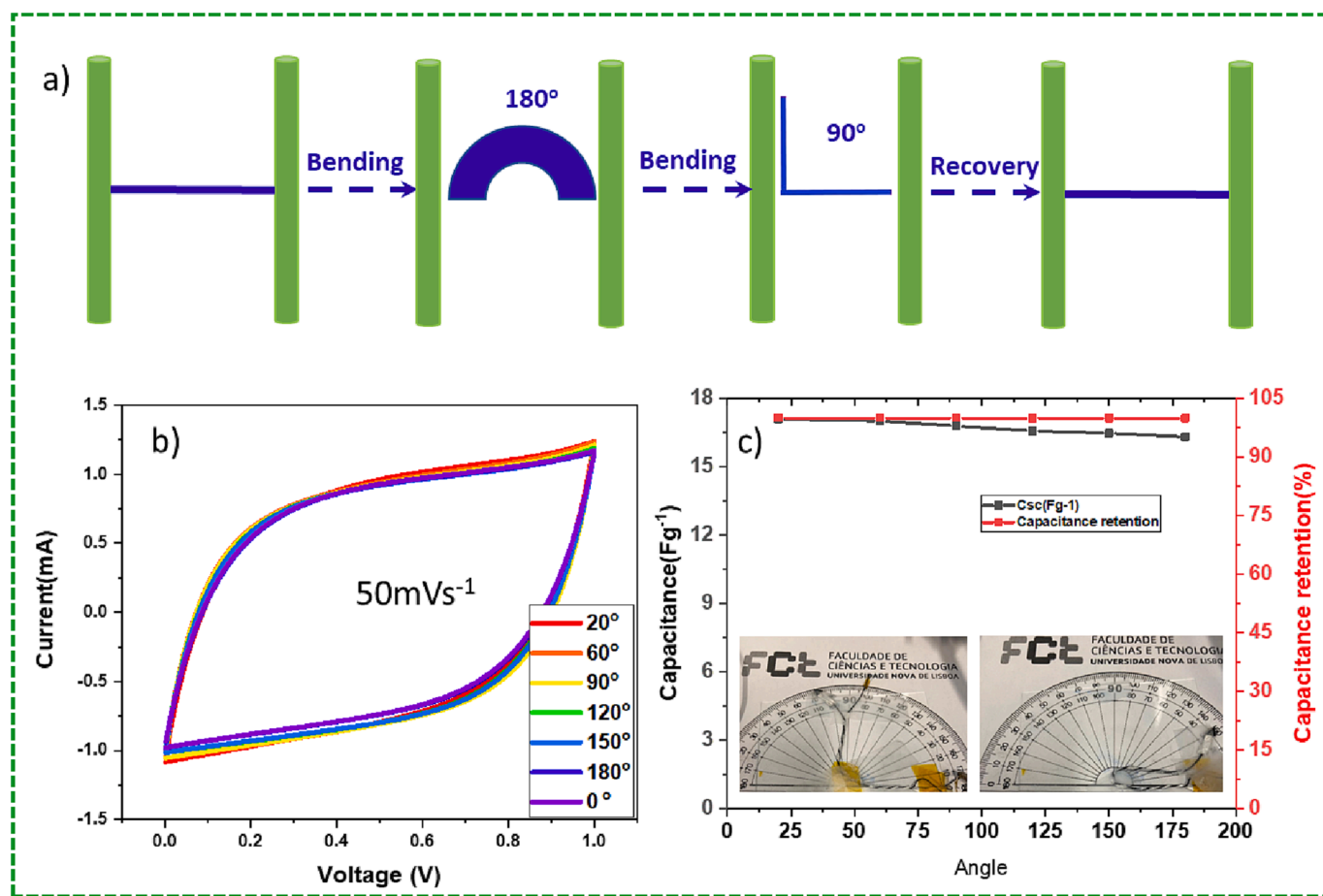
Fig. 7. Bending stability test a) schematic of the imposed bending angles to assess the flexibility of the devices, inset shows the pictorial demonstration of bending of the devices, b-c) shows the comparison of CVs recorded at different angles and corresponding capacitance and capacitance retention, inset shows the pictorial demonstration of bending of the devices.

subjected to a total of 600 abrasion cycles the electrochemical performance of the device was evaluated afterwards and the devices demonstrated excellent abrasion stability even capacitance has increased as compared to the default device. This can be caused by an increase in contact area between electrodes and electrolyte. Similarly, in the Whyzenbeek modified test, fabric is manually rubbed back and forth on the textile integrated devices and the electrochemical performance of the device is evaluated. The capacitances of the devices in both cases increased which is ascribed to enhanced contact factor between the

inner and outer electrodes with electrolyte owing to the pressure exerted by roller in the mechanical testing and also during manual testing. It is observed in both cases that the CVs demonstrated an upward shift during the abrasion testing which may be ascribed to the absorption of electrolyte by the abrasion rollers and also due to increase in equivalent series resistance as shown in Fig. 9b and e. After rotation testing the electrolyte was added to overcome its evaporation along time leading to a shift toward a default position, which is evident from CV's shapes. The fabricated devices have demonstrated excellent abrasion resistance with
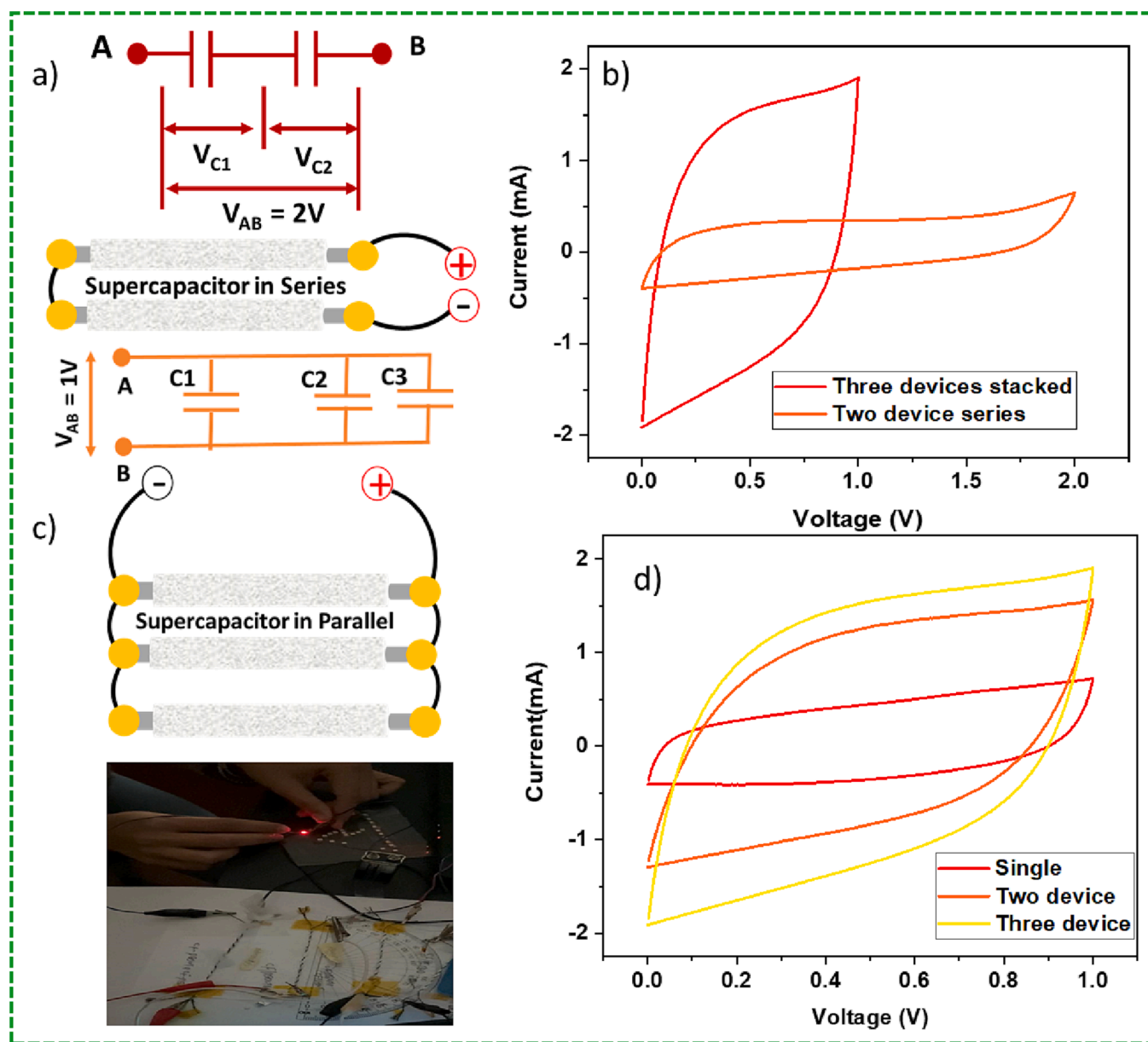
Fig. 8. a-d) Supercapacitors connected in series and stacked in parallel and LED demonstration, a-b) graphical representation of series supercapacitors and corresponding CVs of parallel and series supercapacitors, c-d) graphical demonstration of stacking of three supercapacitors in parallel configuration and corresponding CVs in stacking position along with digital picture demonstration (see video in supporting information).

a complete capacitance retention (100 %) in both methods.

As part of e-textile practical application one of the most important restrictions of incorporating electronic devices in fibrous textiles is its washing resistance. A capacitor device using pristine carbon as electrode and CA: PS 80%:20% as separator was placed in a teabag and immersed in a 100 ml water with 200 μl of soap in a beaker. Then stirring at 200 rpm for 30 min was applied. Before performing this washing, the CV curves of the device were recorded. After 30 min of washing under constant stirring, device was removed and dried under ambient conditions. Then 40 μl SSS electrolyte was added and after washing CV curves were recorded again. Fig. 9g and video demonstration (in supporting information) shows the comparison of the CV curves before and after washing and devices demonstrated an excellent stability after 30 cycles of washing. Cyclic stability tests, for 1000 cycles were also performed and are shown in Fig. 9h-i. Fig. 9i shows the CV curves recorded for different cycles, and it is clear from the graph that device has shown an excellent cyclic stability with above 95% capacitance retention.

4. Conclusions

The blow spinning technique proved to produce quality and stable cellulose-based separators with solution-based composites. Different CA: PS compositions ratios were tested but the results show no influence on the electrochemical performances of the device nor on the blow spinning deposition time, being obtained a suitable membrane in 3 min of deposition. Symmetric fiber-shaped supercapacitors were fabricated with simple carbon yarns and carbon yarns functionalized with PEDOT being chosen CA:PS 80%:20% as greener composition and simulated sweat solution as electrolyte. Specific capacitance of 33 Fg^{-1} was obtained showing the viability of the separator performed by blow spinning, SSS as electrolyte and carbon yarns functionalized with PEDOT. Mechanical resistance to bending and abrasion was evaluated demonstrating that devices had a capacitance retention of above 98 %. Moreover, the washing resistance and cyclic stability was also tested, and results show above 95% of capacitance retention after 30 min soap
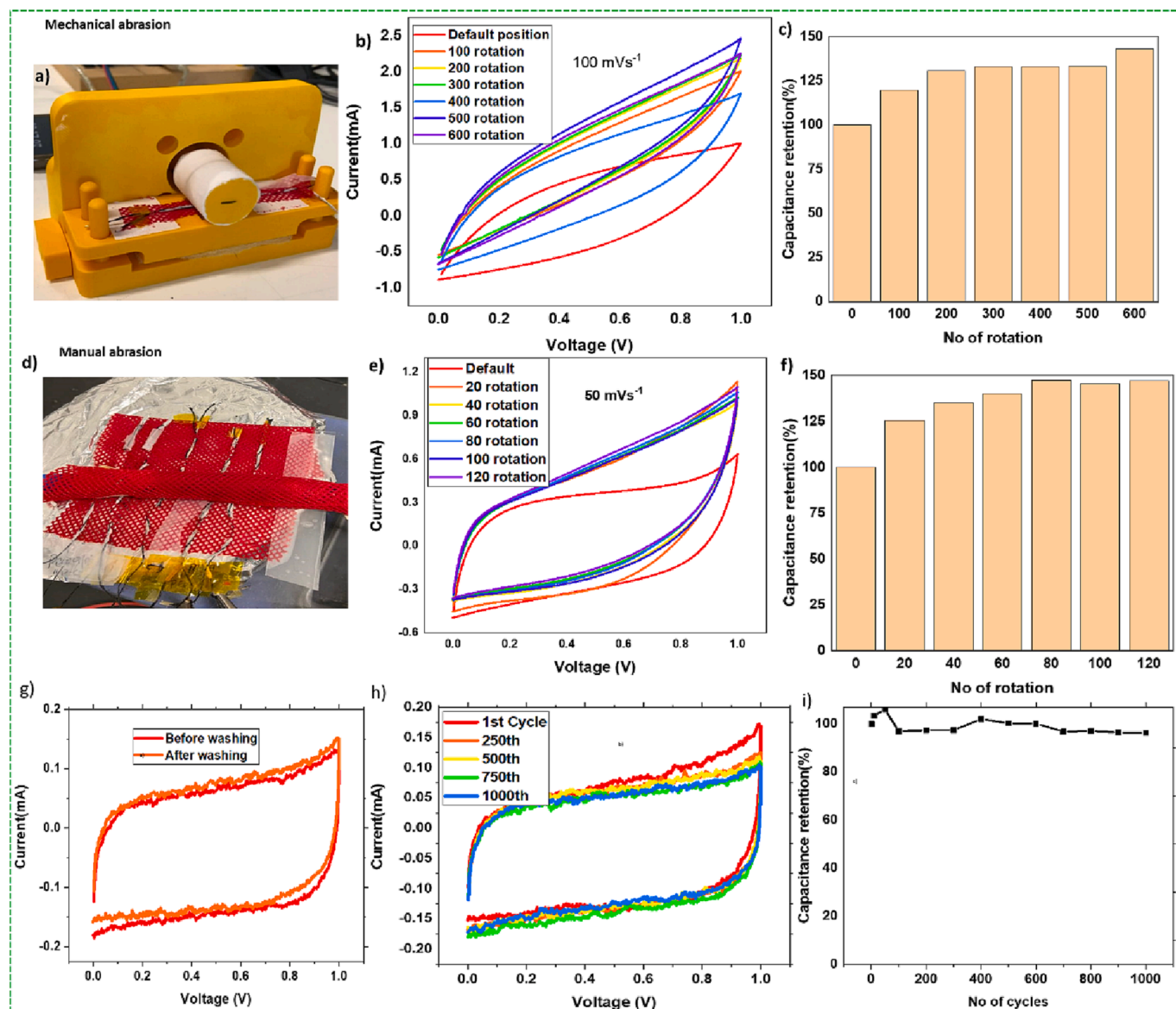
Fig. 9. a) Mechanical abrasion tester, b-c) CVs recorded and corresponding capacitance retention after 600 abrasion rotations, d) manual abrasion tester was performed along the full length of the wire, e-f) CVs and corresponding capacitance retention after 120 rotations of abrasion, g) washing stability of the composite separator, h-i) cyclic stability of the device.

washing procedure and 1000 charge/discharge cycling. The yarn-based supercapacitors herein reported can be one step forward for flexible energy storage devices for E-textile and wearable electronic devices.

Declaration of Competing Interest

The authors declare that they have no known competing financial interests or personal relationships that could have appeared to influence the work reported in this paper.

Data availability

Data will be made available on request.

Acknowledgements

Appendix A. Supplementary data

Supplementary data to this article can be found online at https://doi.org/10.1016/j.cej.2023.142515.

References

[1] C. Chen, L. Hu, Nanocellulose toward advanced energy storage devices: structure and electrochemistry, Acc. Chem. Res. 51 (12) (2018) 3154–3165.

[2] H. Huang, et al., Fabrication of ultrathin, flexible, all-in-one paper supercapacitor with high electrochemical performance based on multi-layer forming in paper sheet formation technology, Chem. Eng. J. 448 (2022), 137589.

[3] B. Dharmasiri, et al., Flexible carbon fiber based structural supercapacitor composites with solvate ionic liquid-epoxy solid electrolyte, Chem. Eng. J. 455 (2023), 140778.

[4] Y. Shi, X. Zhou, G. Yu, Material and structural design of novel binder systems for high-energy, high-power lithium-ion batteries, Acc. Chem. Res. 50 (11) (2017) 2642–2652.

[5] A. Rafique, et al., Recent advances and challenges toward application of fibers and textiles in integrated photovoltaic energy storage devices, Nano-Micro Lett. 15 (1) (2023) 40.

[6] J.W. Choi, D. Aurbach, Promise and reality of post-lithium-ion batteries with high energy densities, Nat. Rev. Mater. 1 (4) (2016) 1–16.

[7] L. Jabbour, et al., Aqueous processing of cellulose based paper-anodes for flexible Li-ion batteries, J. Mater. Chem. 22 (7) (2012) 3227–3233.

[8] Z. Wang, et al., Cellulose-based supercapacitors: material and performance considerations, Adv. Energy Mater. 7 (18) (2017) 1700130.

[9] Z. Wang, et al., Why cellulose-based electrochemical energy storage devices? Adv. Mater. 33 (28) (2021), 2000892.

[10] M. Mahalakshmi, et al., Characterization of biopolymer electrolytes based on cellulose acetate with magnesium perchlorate (Mg (ClO4) 2) for energy storage devices, J. Sci.: Adv. Mater. Devices 4 (2) (2019) 276–284.

[11] Z. Zhang, et al., Cellulose-based material in lithium-sulfur batteries: A review, Carbohydr. Polym. 255 (2021), 117469.

[12] T. Zhang, et al., Recent advances of cellulose-based materials and their promising application in sodium-ion batteries and capacitors, Small 14 (47) (2018), 1802444.

[13] J. Sheng, R. Wang, R. Yang, Physicochemical properties of cellulose separators for lithium ion battery: Comparison with Celgard2325, Materials 12 (1) (2018) 2.

[14] W. Xiao, J. Liu, C. Yan, Nanofiber/ZrO2-based mixed matrix separator for high safety/high-rate lithium–ion batteries, Chem. Phys. Lett. 686 (2017) 134–139.

[15] D. Xu, et al., Eco-friendly and thermally stable cellulose film prepared by phase inversion as supercapacitor separator, Mater. Chem. Phys. 249 (2020), 122979.

[16] L. Zhang, et al., Vibration of an axially moving jet in a dry spinning process, J. Low Freq. Noise Vib. Active Control 38 (3–4) (2019) 1125–1131.

[17] R. Rudra, V. Kumar, P.P. Kundu, Acid catalysed cross-linking of poly vinyl alcohol (PVA) by glutaraldehyde: effect of crosslink density on the characteristics of PVA membranes used in single chambered microbial fuel cells, RSC Adv. 5 (101) (2015) 83436–83447.

[18] F. Jiang, et al., Bacterial cellulose nanofibrous membrane as thermal stable separator for lithium-ion batteries, J. Power Sources 279 (2015) 21–27.

[19] H. Liao, et al., Novel cellulose aerogel coated on polypropylene separators as gel polymer electrolyte with high ionic conductivity for lithium-ion batteries, J. Membr. Sci. 514 (2016) 332–339.

[20] J. Yan, D.-G. Yu, Smoothening electrospinning and obtaining high-quality cellulose acetate nanofibers using a modified coaxial process, J. Mater. Sci. 47 (20) (2012) 7138–7147.

[21] Z. Pang, et al., A room temperature ammonia gas sensor based on cellulose/TiO2/PANI composite nanofibers, Colloids Surf., A Physicochem. Eng. Asp. 494 (2016) 248–255.

[22] H. Sehaqui, et al., Cationic cellulose nanofibers from waste pulp residues and their nitrate, fluoride, sulphate and phosphate adsorption properties, Carbohydr. Polym. 135 (2016) 334–340.

[23] K. Yamaguchi, et al., Highly dispersed nanoscale hydroxyapatite on cellulose nanofibers for bone regeneration, Mater. Lett. 168 (2016) 56–61.

[24] C. Yang, et al., Flexible highly specific capacitance aerogel electrodes based on cellulose nanofibers, carbon nanotubes and polyaniline, Electrochim. Acta 182 (2015) 264–271.

[25] H. Zhu, et al., Wood-derived materials for green electronics, biological devices, and energy applications, Chem. Rev. 116 (16) (2016) 9305–9374.

[26] G. Teng, et al., Renewable cellulose separator with good thermal stability prepared via phase inversion for high-performance supercapacitors, J. Mater. Sci. Mater. Electron. 31 (10) (2020) 7916–7926.

[27] L. Li, et al., Flexible double-cross-linked cellulose-based hydrogel and aerogel membrane for supercapacitor separator, J. Mater. Chem. A 6 (47) (2018) 24468–24478.

[28] D. Boriboon, et al., Cellulose ultrafine fibers embedded with titania particles as a high performance and eco-friendly separator for lithium-ion batteries, Carbohydr. Polym. 189 (2018) 145–151.

[29] M. Bolloli, et al., Nanocomposite poly (vynilidene fluoride)/nanocrystalline cellulose porous membranes as separators for lithium-ion batteries, Electrochim. Acta 214 (2016) 38–48.

[30] T. Yvonne, et al., Properties of electrospun PVDF/PMMA/CA membrane as lithium based battery separator, Cellulose 21 (4) (2014) 2811–2818.

[31] W. Chen, et al., Electrospun flexible cellulose acetate-based separators for sodium-ion batteries with ultralong cycle stability and excellent wettability: the role of interface chemical groups, ACS Appl. Mater. Interfaces 10 (28) (2018) 23883–23890.

[32] Q. Yao, et al., One step construction of nitrogen–carbon derived from bradyrhizobium japonicum for supercapacitor applications with a soybean leaf as a separator, ACS Sustain. Chem. Eng. 6 (4) (2018) 4695–4704.

[33] R. Pan, et al., Mesoporous Cladophora cellulose separators for lithium-ion batteries, J. Power Sources 321 (2016) 185–192.

[34] M. Wojasiński, M. Pilarek, T. Ciach, Comparative studies of electrospinning and solution blow spinning processes for the production of nanofibrous poly (L-lactic acid) materials for biomedical engineering, Polish J. Chem. Technol. 16 (2) (2014).

[35] E.S. Medeiros, et al., Solution blow spinning: A new method to produce micro-and nanofibers from polymer solutions, J. Appl. Polym. Sci. 113 (4) (2009) 2322–2330.

[36] J.E. Oliveira, et al., Nano and submicrometric fibers of poly (D, L-lactide) obtained by solution blow spinning: Process and solution variables, J. Appl. Polym. Sci. 122 (5) (2011) 3396–3405.

[37] J. Li, et al., Promising free-standing polyimide membrane via solution blow spinning for high performance lithium-ion batteries, Ind. Eng. Chem. Res. 57 (36) (2018) 12296–12305.

[38] J. Deng, et al., Cross-linked cellulose/carboxylated polyimide nanofiber separator for lithium-ion battery application, Chem. Eng. J. 433 (2022), 133934.

[39] H. An, C. Shin, G. Chase, Ion exchanger using electrospun polystyrene nanofibers, J. Membr. Sci. 283 (1–2) (2006) 84–87.

[40] H. Kaya, C. Kaynak, J. Hacaloglu, Thermal degradation of polystyrene composites. Part II. The effect of nanoclay, J. Anal. Appl. Pyrol. 120 (2016) 194–199.

[41] F. Liu, X. Chuan, Recent developments in natural mineral-based separators for lithium-ion batteries, RSC Adv. 11 (27) (2021) 16633–16644.

[42] N.A. Khoso, et al., Controlled template-free in-situ polymerization of PEDOT for enhanced thermoelectric performance on textile substrate, Org. Electron. 75 (2019), 105368.

[43] C. Callewaert, et al., Artificial sweat composition to grow and sustain a mixed human axillary microbiome, J. Microbiol. Methods 103 (2014) 6–8.

[44] J.H. Jo, et al., Nature-derived cellulose-based composite separator for sodium-ion batteries, Front. Chem. 8 (2020) 153.

[45] P.K. Sow, R. Singhal, Sustainable approach to recycle waste polystyrene to high-value submicron fibers using solution blow spinning and application towards oil-water separation, J. Environ. Chem. Eng. 8 (2) (2020), 102786.

[46] D.T. Wong, et al., Relationship between morphology and conductivity of block-copolymer based battery separators, J. Membr. Sci. 394 (2012) 175–183.

[47] C. Marchioli, M. Fantoni, A. Soldati, Orientation, distribution, and deposition of elongated, inertial fibers in turbulent channel flow, Phys. Fluids 22 (3) (2010), 033301.

[48] C.L. Casper, et al., Controlling surface morphology of electrospun polystyrene fibers: effect of humidity and molecular weight in the electrospinning process, Macromolecules 37 (2) (2004) 573–578.

[49] S. Srinivasan, et al., Solution spraying of poly (methyl methacrylate) blends to fabricate microtextured, superoleophobic surfaces, Polymer 52 (14) (2011) 3209–3218.

[50] M. Rajesh, et al., A high performance PEDOT/PEDOT symmetric supercapacitor by facile in-situ hydrothermal polymerization of PEDOT nanostructures on flexible carbon fibre cloth electrodes, Mater. Today Energy 6 (2017) 96–104.

[51] A.C. Baptista, et al., Electronic control of drug release from gauze or cellulose acetate fibres for dermal applications, J. Mater. Chem. B 9 (16) (2021) 3515–3522.

[52] N. Lima, et al., Carbon threads sweat-based supercapacitors for electronic textiles, Sci. Rep. 10 (1) (2020) 1–9.

[53] X. Chiu, J. Travis-Sejdic, R.P. Cooney, G.A. Bowmaker, J. Raman Spectros, 2006. 37: p. 1354-1361.

[54] Y. Chen, et al., Enhanced electrochemical performance of PEDOT film incorporating PEDOT:PSS. 2015 2nd International Conference on Machinery, Materials Engineering, Chemical Engineering and Biotechnology, Atlantis Press, 2015.

[55] L. Ortega, et al., Self-powered smart patch for sweat conductivity monitoring, Microsyst. Nanoeng. 5 (1) (2019) 1–10.

[56] D. Wu, et al., A high-safety PVDF/Al 2 O 3 composite separator for Li-ion batteries via tip-induced electrospinning and dip-coating, RSC Adv. 7 (39) (2017) 24410–24416.

[57] W. Kang, et al., Electrospun cellulose acetate/poly (vinylidene fluoride) nanofibrous membrane for polymer lithium-ion batteries, J. Solid State Electrochem. 20 (2016) 2791–2803.

[58] J. Cui, et al., Composite of polyvinylidene fluoride–cellulose acetate with Al (OH) 3 as a separator for high-performance lithium ion battery, J. Membr. Sci. 541 (2017) 661–667.

[59] Q. Xu, et al., Polydopamine-coated cellulose microfibrillated membrane as high performance lithium-ion battery separator, RSC Adv. 4 (16) (2014) 7845–7850.

[60] R. Pan, et al., Nanocellulose modified polyethylene separators for lithium metal batteries, Small 14 (21) (2018) 1704371.

[61] H. Zhang, et al., Nanofibrillated cellulose (NFC) as a pore size mediator in the preparation of thermally resistant separators for lithium ion batteries, ACS Sustain. Chem. Eng. 6 (4) (2018) 4838–4844.

[62] W. Chen, et al., Porous cellulose diacetate-SiO2 composite coating on polyethylene separator for high-performance lithium-ion battery, Carbohydr. Polym. 147 (2016) 517–524.

[63] Y. Zhu, et al., Natural macromolecule based carboxymethyl cellulose as a gel polymer electrolyte with adjustable porosity for lithium ion batteries, J. Power Sources 288 (2015) 368–375.

[64] R. Goncalves, et al., Mesoporous cellulose nanocrystal membranes as battery separators for environmentally safer lithium-ion batteries, ACS Appl. Energy Mater. 2 (5) (2019) 3749–3761.

[65] A.B. Ganganboina, A. Dutta Chowdhury, R.-A. Doong, New avenue for appendage of graphene quantum dots on halloysite nanotubes as anode materials for high performance supercapacitors, ACS Sustain. Chem. Eng. 5 (6) (2017) 4930–4940.

[66] D. Salinas-Torres, et al., Asymmetric hybrid capacitors based on activated carbon and activated carbon fibre–PANI electrodes, Electrochim. Acta 89 (2013) 326–333.

[67] W.-C. Chen, T.-C. Wen, H. Teng, Polyaniline-deposited porous carbon electrode for supercapacitor, Electrochim. Acta 48 (6) (2003) 641–649.

[68] Z. Tabti, et al., Tailoring the surface chemistry of activated carbon cloth by electrochemical methods, ACS Appl. Mater. Interfaces 6 (14) (2014) 11682–11691.

[69] A. Rafique, et al., Flexible wire-based electrodes exploiting carbon/ZnO nanocomposite for wearable supercapacitors. 23(7) (2017)1839-1847.

[70] L. Manjakkal, et al., A wearable supercapacitor based on conductive PEDOT: PSS-coated cloth and a sweat electrolyte, Adv. Mater. 32 (24) (2020) 1907254.

[71] L. Manjakkal, et al., Flexible supercapacitor with sweat equivalent electrolyte for safe and ecofriendly energy storage. 2020 IEEE International Conference on Flexible and Printable Sensors and Systems (FLEPS), IEEE, 2020.

[72] J. Lv, et al., Sweat-based wearable energy harvesting-storage hybrid textile devices, Energ. Environ. Sci. 11 (12) (2018) 3431–3442.

[73] S. Selvam, Y.K. Park, J.H. Yim, Design and testing of autonomous chargeable and wearable sweat/ionic liquid-based supercapacitors, Adv. Sci. 9 (25) (2022) 2201890.

[74] D. Dahlan, et al., Effect of TiO2 on duck eggshell membrane as separators in supercapacitor applications. Materials Science Forum, Trans Tech Publ, 2015.

[75] G.E. Spina, et al., Natural polymers for green supercapacitors, Energies 13 (12) (2020) 3115.

[76] X. Zhang, et al., Solid-state, flexible, high strength paper-based supercapacitors, J. Mater. Chem. A 1 (19) (2013) 5835–5839.